Two Distinct Types of CME-Flare Relationships based on SOHO and STEREO observations

Soojeong Jang, Graduate student
Kyung Hee University, Korea

Abstract

In this paper we present two distinct types of CME-flare relationships according to their observing time differences using 107 events from 2010 to 2013. The observing time difference, ΔT, is defined as flare peak time minus CME first appearance time at STEREO COR1 field of view. There are 41 events for group A ($\Delta T < 0$) and 66 events for group B ($\Delta T \geq 0$). We compare CME 3D parameters (speed and kinetic energy), which is calculated by the Stereoscopic CME analysis tool (StereoCAT) provided by NASA CCMC, and their associated flare properties (peak flux, fluence, and duration). Our main results are as follows. First, there are better relationships between CME and flare parameters for group B than that of group A. Especially, CME 3D kinetic energy for group B is well-correlated with flare fluence with the correlation coefficient of 0.67, which is much stronger than that (cc=0.31) of group A. Second, the events belonging to group A have short flare durations less than 1 hour (mean=21mins), while the events for group B have longer durations up to 4 hours (mean=81mins). Third, the mean value of height at peak speed for group B is 4.05 Rs, which is noticeably higher than that of group A (1.89 Rs). These results indicate a closer relationship between CME rising motions and magnetic reconnection process in a flare, especially for group B.

1. INTRODUCTION

Coronal Mass Ejections (CMEs) are one of the major eruptive phenomena of the Sun and emit a large amount of energy into the interplanetary space. Especially front-side halo CMEs are main causes of heliospheric and geomagnetic disturbances (St. Cyr et al. 2000; Webb et al. 2000; Kim et al. 2005; Moon et al. 2005). It is well known that the halo CMEs are accompanied by solar flares (Munro et al. 1979; Harrison 1995; Aarnio et al. 2011) and their triggering mechanism is magnetic reconnection, which is explained by solar eruption models, e.g. the standard CME-flare model (CSHKP; Carmichael 1964; Sturrock 1968; Hirayama 1974; Kopp & Pneuman 1976).

Over two decades, there have been many studies on the comparison between CME properties observed by coronagraphs and its-associated flare ones observed by Geostationary Operational Environmental Satellite (GOES). Using the 249 events observed by the Solar Maximum Mission (SMM), Hundhausen (1997) reported the relationship between CME kinetic energy and integrated soft Xray (SXR) flux (i.e., fluence) with a correlation value of 0.53. According to results from Moon et al. (2002), there is a positive correlation (cc=0.47) between speeds of limb CMEs observed by the Large Angle Spectroscopic Coronagraph (LASCO; Brueckner et al. 1995) on board the SOlar and Heliospheric Observatory (SOHO: 1997～) and integrated SXR fluxes from 1996 and 2002. Burkepile et al. (2004) found that the correlation coefficient between CME kinetic energy and flare peak flux is 0.74 for 24 limb CMEs which had both speed and mass. Vršnak et al. (2005) also presented that the CME speed and width increase with flare strength. They introduced a proxy of CME kinetic energy, which is defined as a square of average speed multiplied by an angular width of CME, and found that the correlation between this proxy and integrated SXR flux is 0.47. Bein et al. (2012) reported a weak positive correlation between CME peak speed observed by the Solar TErrestrial RElations Observatory (STEREO; Kaiser et al. 2008) and flare peak flux (cc=0.32). Summing up, the correlation value between CME speed (or kinetic energy) and flare strength (or fluence) ranges from 0.32 to 0.74, which depends only on whether only limb events are considered or not. And all these results are based on that CME properties are obtained by single coronagraph.

In this paper, we want to make a new attempt to obtain better relationships between CMEs and flares with the following two perspectives. First, we use the three-dimensional (3D) parameters of CMEs to reduce the projection effect of CME properties. STEREO makes it possible to determine the CME 3D parameters (speed, width, etc) by applying the stereoscopic method based on multi-view observations (Thernisien et al. 2009; Liu et al. 2010; Millward et al. 2013). According to quadratic observations between SOHO and STEREO, Several researchers found that apparent angular widths observed from SOHO LASCO and STEREO COR2 are quite different from each other (Gopalswamy et al. 2012; Lee et al. 2015). Using 306 frontside halo (partial and full) CMEs from 2009 to 2013, Jang et al. (2016) presented statistical comparison between CME projected two-dimensional (2D) parameters from single coronagraph (LASCO) and 3D ones from multi coronagraph (STEREO A and B), which is calculated by stereoscopic CME analysis tool (StereoCAT) provided by NASA Community Coordinated Modeling Center (CCMC). They found that projected speeds tend to be approximately 20% underestimated when compared with 3D speeds. They also found that the apparent angular width of a halo CME seen by SOHO is quite differ from its 3D width, which ranges from 30° to 158°. Until now, there has been no comprehensive study on the comparison between CME

3D parameters and flare ones. Second, we use the data from COR1 of the Sun Earth Connection Coronal and Heliospheric Investigation (SECCHI; Howard et al. 2008) onboard STEREO, which covers from 1.4 to 4 solar radii, to investigate the propagation of CMEs in low corona. It is hard to measure a CME start time using direct observations, because low coronal region is hidden by occulters of coronagraphs. A typical method to estimate a CME start time is a height-time extrapolation with assumption of a constant speed or acceleration (Zhang et al. 2002; Mickalek 2009; Youssef et al. 2013). This is still not accurate because there are several phases of CME evolution with different speeds in the low corona (Zhang & Dere 2006). Here, we directly use the first appearance times and heights from COR1 data.

In this paper, we make a comparison between CME 3D parameters from multi-spacecraft and its associated flare ones according to their observational time difference between flare peak time on X-ray flux and CME first appearance time at COR1. In Section 2, we explain our data set and observing time differences. Then our results and discussion are present in Section 3. A brief summary and conclusion are delivered in Section 4.

2. DATA AND METHOD

To compare between the CME 3D parameters and its associated flare ones, we use data taken from our previous study (Jang et al. 2016), which are 306 LASCO front-side halo CMEs (apparent angular width ≥ 120°) from 2009 to 2013. These CMEs are well-observed by both SOHO and STEREO A&B and their structures are clearly seen in more than 2 coronagraph data among the three spacecraft. These CMEs have two-dimensional (2D) CME parameters, which are directly taken from SOHO LASCO CME catalog (Yashiro et al. 2004)[1], as well as three-dimensional (3D) ones. To estimate CME 3D parameters, we use the STEREO CME analysis tool (StereoCAT[2]) based on a triangulation method, which is provided by CCMC at NASA (see Mays et al. 2015, and references therein). The CME 3D speed we used is an average value which tried several times. Figure 1 shows a snapshot of the StereoCAT-applied STEREO A and B coronagraphs. And flare parameters (peak flux, fluence, and duration) are taken from National Geophysical Data Center (NGDC) flare list[3].

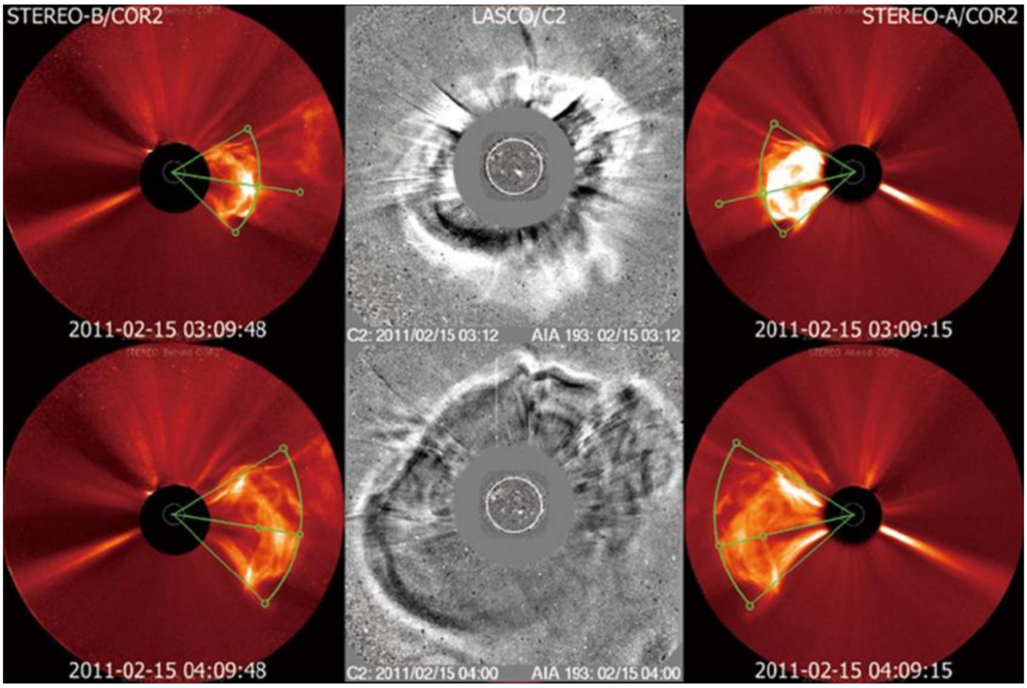

Figure 1. Successive coronagraph images of the 2011 February 15 CME observed by STEREO B (left), SOHO (middle), and STEREO A (right). The green lines in the STEREO coronagraph images indicate fittings of the CME by StereoCAT.

Among 306 events, we choose 107 flare-associated CMEs with the following criteria. (1) We pick out flares which start within 2 hours of the CME first observing times in LASCO C2. (2) We checked movies obtained by the Atmospheric Imaging Assembly (AIA; Lemen et al. 2012), 193 and 304 Å, on board Solar Dynamics Observatory (SDO) and the Extreme Ultraviolet Imager (EUVI; Wuelser et al. 2004), 195 and 304 Å, on board STEREO to find bright features or any kind of eruption signatures. (3) If there are several flares during the time

---

[1] http://cdaw.gsfc.nasa.gov/CME_list/
[2] http://ccmc.gsfc.nasa.gov/analysis/stereo/
[3] ftp.ngdc.noaa.gov/STP/SOLAR_DATA/SOLAR_FLARES/FLARES_XRAY

window, we carefully inspect the evolution of SDO and coronagraph images and determine the corresponding flare, which all correspond to the largest flares. (4) Only flares observed within ±70° longitude seen by SDO AIA are considered because the time integrated SXR flux (i.e. fluence) might be underestimated if some brightening features are located near or behind the limb. The events we used are 14 X-class flares, 44 M-class flares, 44 C-class flares and 5 B-class flares.

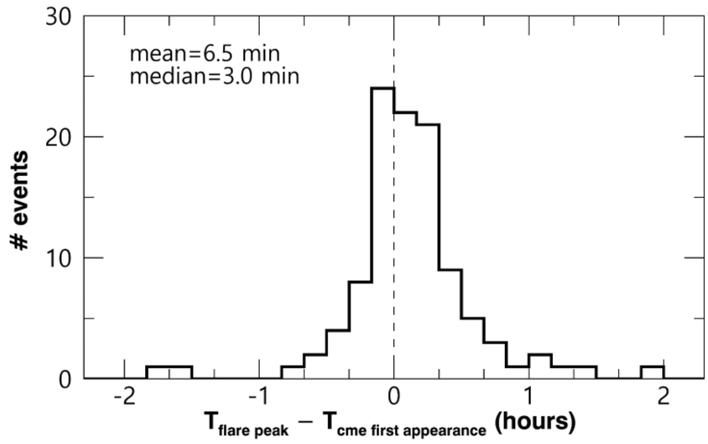

Figure 2. Histogram of observing time differences between flare peak time and CME first appearance time in the STEREO COR1 field-of-view. Mean and median values are 6.5 and 3 minutes, respectively. Vertical dashed line indicates that time difference is zero.

In this study, we use the CME first appearance time using STEREO COR1 which can observe low corona between 1.4 and 4 Rs (Howard et al. 2008). Besides, it has a high time cadence of 2.5 minute (sometimes 5 minute). Here we define the observing time difference, ΔT, as flare peak time minus CME first appearance time. According to this observing time difference, we divide the data into two different groups. A negative value of time difference ($\Delta T<0$), called group A, indicates that a CME first appears in the COR1 field-of-view after its-associated flare peak time. Whereas, a positive value ($\Delta T \geq 0$) as group B implies that a CME first appears before the flare peak time. Figure 2 shows a histogram of the time differences for 107 events. Among them, there are 41 events for group A and 66 events for group B. This histogram approximately follows a normal distribution, with mean and median values are 6.5 and 3 minutes, respectively.

3. RESULT AND DISCUSSION

We compare CME 2D and 3D parameters, such as speed and kinetic energy, with parameters of their associated flares. Although all CME parameters have meaningful relationships with two flare parameters (peak flux and fluence), there are better correlations of CME parameters with fluence than those with peak flux. Hereafter we show relationships of CME parameters and fluence.

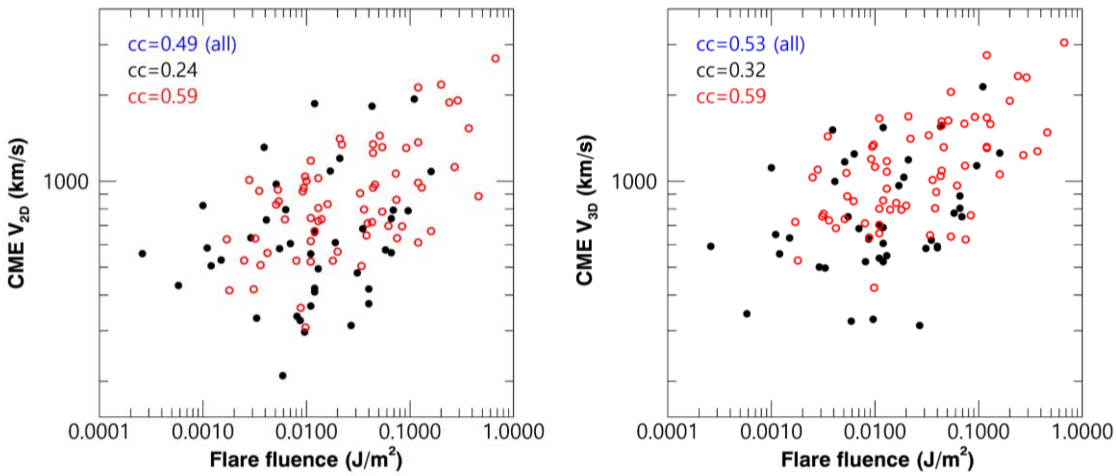

Figure 3. The relationship between CME speed and flare fluence: 2D (left) and 3D speed (right). Black closed and red open circles indicate results for group A and B, respectively.

Figure 3 shows a comparison between CME speeds and flare fluences. A correlation coefficient (0.53) between the 3D speed (V_{3D}) and the fluence for all events is slightly higher than that (0.49) between the 2D speed (V_{2D}) and the fluence. These coefficients are somewhat higher than the results of Moon et al. (2002), who showed correlation coefficient (0.47) between the 2D speed and the flare fluence for the limb events observed from 1996 to 2000. Our results are smaller than Salas-Matamoros & Klein (2015) who found that correlation coefficient is 0.58 using 49 limb CMEs observed from 1996 to 2008. It is noted that the linear relationship (cc=0.59) between the 3D speed and the fluence for group B is much more clear than that (cc=0.32) for group A, which is also seen in the case of 2D speed.

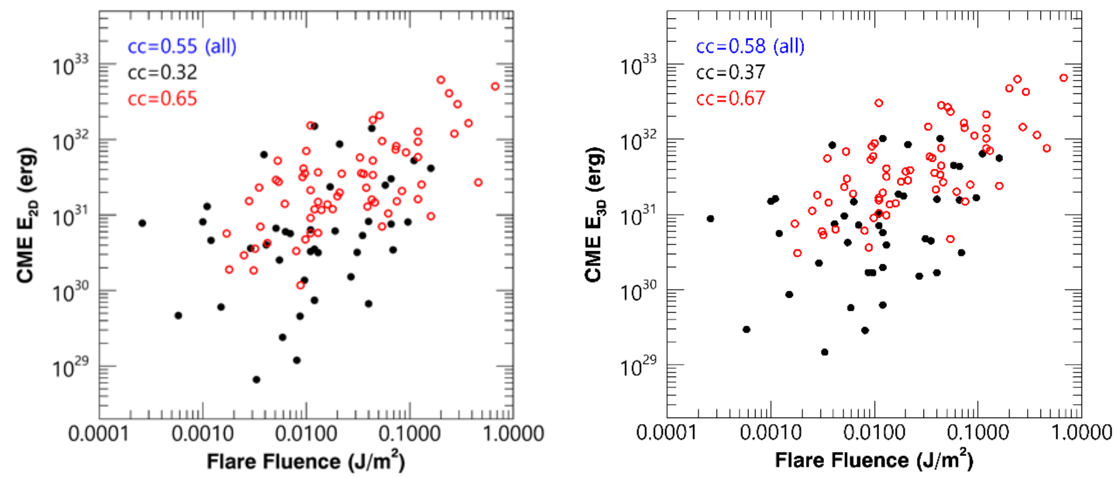

Figure 4. The relationship between CME kinetic energy and flare fluence: 2D (left) and 3D kinetic energies (right). Black closed and red open circles indicate results for group A and B, respectively.

We compare CME kinetic energy and flare fluence in Figure 4. The CME 2D speed to calculate 2D kinetic energy (E_{2D}), and similarly 3D kinetic energy (E_{3D}) comes from 3D speed. Because all the events are halo CMEs seen by LASCO, masses of CMEs measured by LASCO may have large uncertainties. We find that correlation coefficients between CME kinetic energy and flare fluence for all events are 0.55 and 0.58 for 2D and 3D, respectively. These values are quite similar to result from Yashiro & Gopalswany (2009) who found that correlation between CME 2D kinetic energy and fluence is 0.56 using CMEs observed from 1996 to 2007. Especially, the correlation coefficient between 3D kinetic energy and flare fluence for group B is 0.67, which is much higher than that (0.39) for group A. This kind of noticeable difference between two groups is also seen in 2D case.

Table 1. Correlation coefficients between CME and flare parameters, and their p-values.

	Peak flux						Fluence					
	All		Group A		Group B		All		Group A		Group B	
	cc	p-value	cc	p-value	cc	p-value	cc	p-value	cc	p-value	cc	p-value
V_{2D}	0.29	0.002	0.16	0.306	0.51	<0.001	0.49	<0.001	0.24	0.128	0.59	<0.001
V_{3D}	0.30	0.001	0.22	0.171	0.54	<0.001	0.53	<0.001	0.32	0.043	0.59	<0.001
E_{2D}	0.30	0.002	0.28	0.075	0.56	<0.001	0.55	<0.001	0.32	0.038	0.65	<0.001
E_{3D}	0.30	0.001	0.32	0.041	0.58	<0.001	0.58	<0.001	0.37	0.015	0.67	<0.001

We summarize the correlation coefficients between CME and flare parameters, and their p-values in Table 1. The p-value means a probability to occur by chance when both quantities are randomly distributed, which depends on correlation coefficient and the number of data. Commonly, p-value<0.05 means that this relationship is statistically significant. All CME parameters have meaningful relationships with two flare parameters (peak flux and fluence), since all corresponding p-values are smaller than 0.05. It is noted that correlations of CME parameters with flare fluence for all events are quite higher than those with flare peak flux. For example, the correlation coefficient (cc=0.58) of CME 3D kinetic energy with fluence is noticeably larger than that (cc=0.30) with flux. This tendency is also found for the other CME parameters as well. This fact implies that flare fluence might be a better proxy for flaring energy than flare peak flux since it is an integration of GOES flux from flare starting time to end time. According to previous studies (Yashiro & Gopalswany 2009; Salas-Matamoros & Klein 2015), it is also found that a correlation coefficient of CME parameter (speed or kinetic energy) with flare fluence is a little higher than that with flare peak flux. In this study, we find that the correlations of 3D CME parameters with flare fluence, are equal to or a little higher than those of 2D values. Especially, it is noted that there are much better correlations between CME and flare parameters for group B than those for group A. The corresponding p-values for group B are all smaller than 0.001, which means that all these relationships are statistically significant. On the other hands, the p-values for group A are much greater than those for group B, and one p-value is larger than 0.05, which implies statistically insignificant.

As the other flare parameters, we investigate flare durations (T_{flare}) of the events. T_{flare} is defined as a time interval from flare start to end time. T_{flare} for group A are all less than 1 hour, which ranges from 6 and 53 minutes with mean values of 21 minutes. While T_{flare} for group B vary from 10 minutes to up to 4 hours with mean values of 81 minutes. Long duration flares ($T_{flare} \geq 1$ hour) are only occurred in group B. We make a comparison between CME 3D kinetic energy and T_{flare} shown in Figure 5. We find that CME 3D kinetic energy tends to increase with its associated T_{flare}. Their correlation coefficient is 0.42 and its p-value is less than 0.05. There are events for only group B with high 3D kinetic energy bigger than approximately 1×10^{32} erg. The events with small kinetic energy less than $\times10^{30}$ erg are only for group A.

According to previous studies (Sheeley et al. 1983; Yashiro & Gopalswany 2009), long duration flares are likely to be associated with CMEs. Therefore we also check by dividing CME-flare events into two groups according to flare duration (T_{flare}): short duration (< 1hour) and long duration (≥ 1hour) groups. The correlation coefficients between CME 3D kinetic energy and flare fluence for long and short duration groups are 0.72 and 0.52, respectively. The difference between these coefficients is smaller than that between two values based on ΔT (Figure 4). Even though most of the X-class flares seem to be intimately associated with CMEs, their durations are all within 1 hour with the mean value of 35 minutes. According to our classification, six events among X-class events (6/14) belong to group B and the other events (8/14) are in group A. In this respect, the classification based on ΔT seems to more useful to separate whether the CME-flare relationship is close or not.

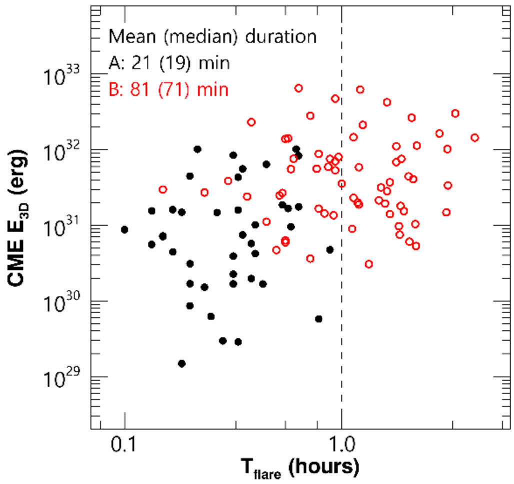

Figure 5. CME 3D speed plotted against flare duration. Vertical dashed line indicates the flare duration as 1 hour.

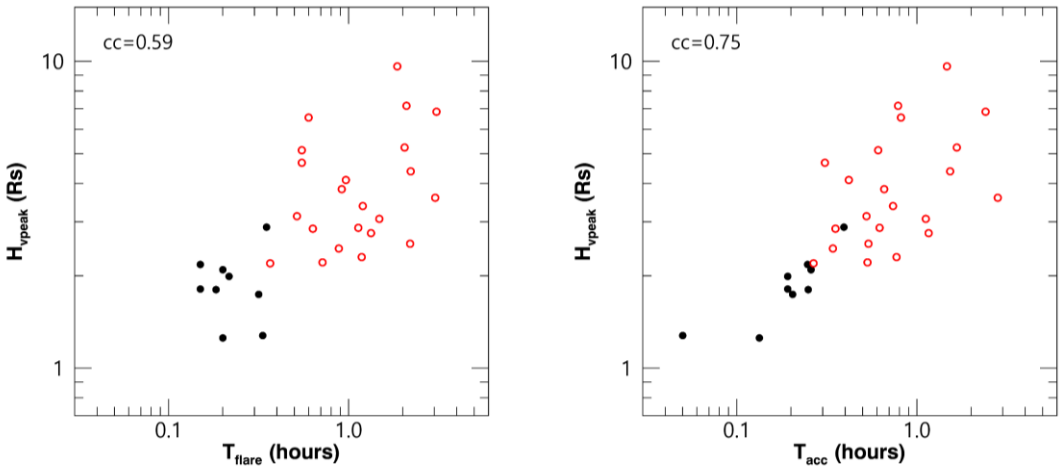

Figure 6. CME peak speed heights of1 limb CMEs shown as a function of flare duration (left) and CME acceleration duration (right). The CME acceleration duration is defined as CME peak speed time minus flare start time. Black closed circles correspond to results of group A and red open circles to those of group B.

We carefully make a comparison between CME speed and GOES X-ray flux profiles. In order to obtain height-time measurements, we use STEREO EUVI 195 ˚*A*, COR1, and COR2. Here the height corresponds to a distance from solar center to CME leading edge. When we measure heights of CME leading edges, we try to do several times in order to reduce the measurements errors and the uncertainties of heights are less than 10%.

In order to minimize the projection effects, we need to select limb CMEs (31 events), whose longitudes are larger than 70°, seen by STEREO A or B. There are 9 events for group A and 22 events for group B. Figure 6 shows comparison between the height at CME peak speed, H_{vpeak}, and two types of durations: its associated flare duration, T_{flare}, and CME acceleration duration, T_{acc}. T_{acc} is assumed as a time interval from the flare start time to the time at CME peak speed, because CME initial acceleration phase synchronize with flare rise phase (Zhang et al. 2001). We find that T_{acc} is very similar to flare rise time with a high correlation coefficient of 0.89. H_{vpeak} of 31 CMEs range from 1.25 to 9.62 Rs with the mean of 3.42 solar radii. There is a general trend that H_{vpeak} increases with T_{flare} and T_{acc} with correlation coefficients of 0.59 and 0.75. The CMEs for group B have higher H_{vpeak} and longer T_{acc} than those of group A. The mean value of H_{vpeak} for group B is 4.05 Rs, which is noticeably higher than that (1.89 Rs) of group A. This means that CMEs for group B are more accelerated until higher H_{vpeak} than those for group A.

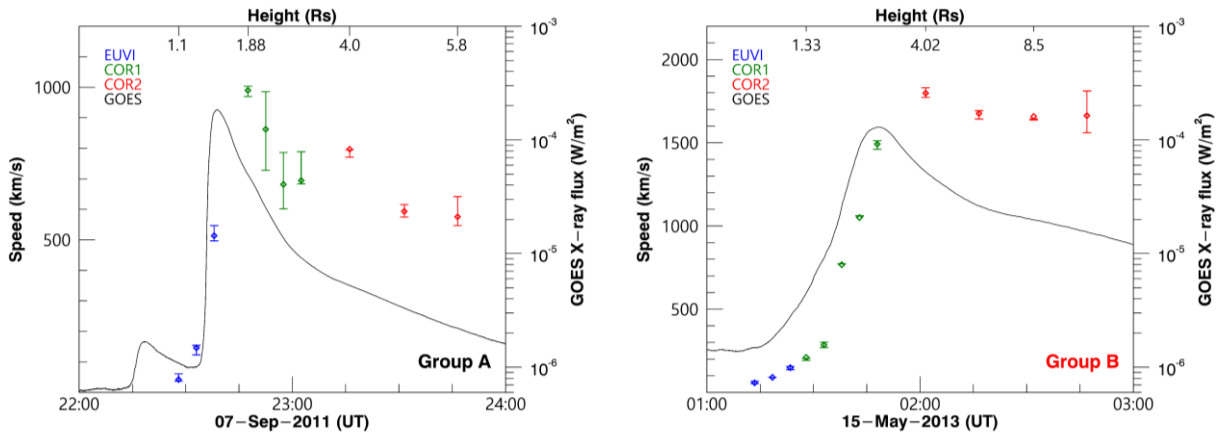

Figure 7. Comparison between GOES X-ray flux and CME speed profiles of two representative examples: 2011 September 7 event (top) for group A and 2013 May 15 event (bottom) for group B. Diamond symbols indicate the CME speed at a given time, which were estimated by a set of STEREO EUVI (blue), COR1 (green), and COR2 (red). Speeds are derived using the height difference between two successive images. The black lines indicate temporal profiles of GOES x-ray fluxes for two X-class flares. The error bars correspond to the minimum and maximum values of several measurements. The measurements of speed were made for only two successive data obtained by the same instrument (e.g., EUVI or coronagraph).

To show more quantitatively the characteristics of two groups, we select two representative events: 2011 September 7 event for group A and 2013 May 15 event for group B (Figure 6). These two events have similar flare strengths (X1.8 for group A event and X1.2 for group B event), however CME 3D speeds are quite different; 751 km/s for group A event and 1667 km/s for group B event. The CMEs for both group A and B are accelerated during flare rise phase. The flare rise time of the first event is 12 minutes, while that of the latter event is 22 minutes. H_{vpeak} of the second one is 4.05 Rs, which is much higher than that (1.85 Rs) of the first one. A closer comparison between CME speed and GOES X-ray flux profile for two representative examples shows that the temporal evolutions of two profiles for group B are consistent with each other for a longer time than that for group A.

4. SUMMARY AND CONCLUSION

We have investigated the CME-flare relationships using 107 halo CMEs from 2010 to 2013 observed by both SOHO and STEREO. To reduce the projection effects, we used the CME 3D parameters calculated by stereoscopic CME analysis tool (StereoCAT). Then we examined the CME-flare relationship for whole events as well as for two distinct groups according to their observing time difference (ΔT). A CME for group A appears in the COR1 field-of-view (ΔT<0) after its-associated flare peak time, while a CME for group B appears before flare peak time (ΔT≥0). We have found that there are much higher correlation coefficients between CME parameters (speed and kinetic energy) and flare fluence for group B than those of group A. The most representative case is that CME 3D kinetic energy for group B is well-correlated with flare fluence (cc=0.67), which is much stronger than that (cc=0.31) of group A. We also summarized the characteristics of CMEs and flares depending on two distinct groups (Table 2). For all events, mean values of CME 3D speed and kinetic energy are 1041 km/s and 6.41×10^{31} erg, respectively. And their associated T_{flare} is 58 minutes on average. We found that events for group B have larger values of CME and flare parameters than those of group A. The CMEs for group B have a higher mean speed (1182 km/s), which is noticeably larger than that (814 km/s) for group A. The mean 3D kinetic energy for group B is about 9×10^{31} erg, which is approximately 5 times higher than that for group A. The mean H_{vpeak} (4.05 Rs) for group B is much higher than that (1.85 Rs) for group A. Similarly, flares for group B have a much longer duration and rise time, which are about 3 times longer than those of group A.

Table 2. Mean (median) values of CME and flare parameters for all events as well as two distinct groups.

Parameters	All	Group A	Group B
CME 3D speed	1041 km/s	814 km/s	1182 km/s
CME 3D kinetic energy	6.41×10^{31} erg	1.96×10^{31} erg	9.17×10^{31} erg
CME height at peak speed*	3.47 Rs	1.85 Rs	4.05 Rs
Flare duration	58 mins	21 mins	81 mins
Flare rise time	30 mins	11 mins	41 mins

*31 limb CMEs seen by STEREO A or B

The intimate relationship between flares and CMEs have been well observed and discussed by several studies (Zhang & Dere 2006; Maričič et al. 2007; Temmer et al. 2010), which insisted that there are the feedback relationship between CME initial acceleration and the flare energy release. According to the conventional CME-flare standard models (Shibata 1996; Lin & Forbes 2000), a current sheet is formed below plasma bubble (i.e., CME) and a magnetic reconnection occurs in the vertical current sheet, which can be stretched by a rising motion of CME. Qiu et al. (2004) found that the total reconnection fluxes from flare observations are related to the CME speeds. Unfortunately, it is hard to directly observe the current sheets associated with flares. The post-CME current sheets have been only reported by several authors (Ko et al. 2003; Raymond et al. 2003; Bemporad 2008). Based on our results (Tables 1 & 2), faster CMEs associated with strong flares for group B tend to have a higher H_{vpeak} and a longer T_{flare}. It is very interesting to note that H_{vpeak} is well correlated with T_{flare} and T_{acc}.

This fact implies that H_{vpeak} should be a proxy of the length of current sheet in CME evolution. A higher H_{vpeak} and a longer T_{acc} of CME for group B could be explained by that magnetic reconnections for group B continuously occur for a longer time than those for group A. These results show that the CMEs for group B are more closely related to flares than those for group A.

REFERENCES

Aarnio et al. 2011, *Sol. Phys.*, 268, 195-212

Bein et al. 2012, ApJ, 738, 191

Bemporad, A. 2008, ApJ, 689, 572

Burkepile et al. 2004, J. Geophys. Res., 109, A03103

Brueckner et al. 1995, *Sol. Phys.*, 162, 357

Carmichael, H. 1964, *NASA Special Publication*, 50, 451

Gopalswamy et al. *Sun and Geophere*, 7(1), 7-11

Harrison, R.A. 1995, *Astron. Astrophys.*, 304, 585

Hirayama, T. 1974, *Sol. Phys.*, 34, 323

Howard et al. 2008, *Space Science Reviews*, 136, 67-115

Hundhausen, A. J. 1997, Coronal mass ejections, in Cosmic Winds and the Heliosphere, edited by J. R. Jokipii, C. P. Sonett, and M. S. Giampapa, p. 259, Univ. of Arizona Press, Tucson.

Jang et al. 2016, ApJ, 821, 95

Kaiser et al. 2008, SSRv, 136, 5-16

Kim et al. 2005, J. Geophys. Res., 110, A11104

Ko et al. 2003, ApJ, 594, 1068

Kopp & Pneuman 1976, *Sol. Phys.*, 50, 85

Lee et al. 2015, J. Geophys. Res., 120, 10237-10249

Lemen et al. 2012, *Sol. Phys.*, 275, 17

Lin & Forbes 2000, J. Geophys. Res., 105, 2375

Liu et al. 2010, ApJ, 722, 1762

Maričič et al. 2007, *Sol. Phys.*, 241, 99

Mays et al. 2015, *Sol. Phys.*, 290, 1775-1814

Mickalek, G. 2009, *A&A*, 494, 263

Moon et al. 2002, ApJ, 581, 694-702

Moon et al. 2005, ApJ, 624, 414-419

Millward et al 2013, *Space Weather*, 11, 57-68

Munro et al 1979, *Sol. Phys.*, 61, 201-215

Qiu et al. 2004, ApJ, 604, 900

Qiu & Yurchyshyn 2006, ApJ, 634, L121-L124

Raymond et al. 2003, ApJ, 597, 1106

Salas-Matamoros & Klein 2015, *Sol. Phys.*, 290, 1337-1353

Shanmugaraju et al. 2011, *Sol. Phys.*, 270, 273

Sheeley et al. 1983, ApJ, 272, 349-354

Shibata, K. 1996, *Adv. Space Res*, 17, 9

Shibata & Magara 2011, *Living Rev. Sol. Phys.*, 8, 6

St. Cyr et al. 2000, J. Geophys. Res., 105(A8), 18169-18185

Sturrock, P. A. 1968, ApJS, 73, 78

Temmer et al. 2010, ApJ, 712, 1410

Thernisien et al. 2009, *Sol. Phys.*, 256, 111-130

Vršnak et al. 2005, *A&A*, 269, 339-346

Webb et al. 2000, J. Geophys. Res., 105(A4), 7491-7508

Wuelser et al. 2004, *Proc. SPIE*, 5171, 111

Yashiro et al. 2004, J. Geophys. Res.109, A07105

Yashiro & Gopalswamy 2009, in IAU Symp. 257, Universal Heliophysical Processes, ed. N. Gopalswamy and D. F. Webb (Cambridge: Cambridge Univ. Press), 233

Youssef et al. 2013, J. Geophys. Res.109, A07105

Zhang et al. 2001, ApJ, 559, 452

Zhang et al. 2002, ApJ, 574, L97

Zhang, J., & Dere, K. P. 2006, ApJ, 649, 1100-1109